

CST0010

Generalized Conforming Triangular Element for Thermal Bending Analysis of Thin Plate

Chatthanon Bhothikhun^{1,*}

¹ Department of Mechanical Engineering, Faculty of Engineering and Industrial Technology,
Silpakorn University, Nakhon Pathom 73000, Thailand

* Corresponding Author: chatthanon@outlook.com, Tel: (+6634) 259 025, Fax: (+6634) 219 367

Abstract

The generalized conforming triangular finite element with nine degrees of freedom for thermal bending analysis of thin plate due to the temperature gradient through its thickness is developed. The finite element formulation with detailed finite element matrices are derived based on the modified potential energy principle and the generalized compatibility conditions. The closed-form of the thermal loading which can be apply directly to the computer program is also derived and express. The effectiveness of the proposed element is evaluated by several examples. Results show that the element exhibits good performance for the analysis of plate bending problem under thermal loading.

Keywords: finite element method, thermal plate bending, generalized conforming, triangular element

1. Introduction

The finite element method has been widely used for the analysis of plate bending problems as the exact solutions of the real applications cannot be derived. The difficulty of the finite element in plate bending is the requirement of C_1 continuity so that the value of transverse deflection w and its slope must impose continuity between elements. Such difficulty brings about various types of plate bending elements which have been developed during the past decades [1-4].

Early developed plate bending elements were the non-conforming element type, such as the well-known BCIZ triangular element [5] which could provide good solution accuracy in plate bending analysis. The element was non-conforming since the normal slope along the element edges cannot be represented by the corner node connections. It was found that the solution obtained from the non-conforming elements sometimes was superior to that obtained from the conforming element type. However, these non-conforming elements sometimes caused divergent results in some problems so that the convergence to the correct result could not be ensured. Meanwhile, the conforming element types were quite complicated to formulate and were found to be too stiff as it imposed excessive conditions of continuity [6]. As a result, these elements generally did not used in the real applications.

Another element type was the thin plate DKT element based on discrete Kirchhoff theory [3]. Although this element provides high solution accuracy [7, 8], the element formulation was quite complicate and the transverse displacement w was defined only along element sides.

Another type of thin plate bending element was the generalized conforming element [9]. The generalized conforming element was formulated based on the modified potential energy principle and the generalized compatibility conditions by using the point

compatibility conditions at each node and the line compatibility conditions along each side [10]. The nine degrees of freedom triangular element GPL-T9 then can be formulated. The result obtained from the element passes the patch test and provides excellent performance. The generalized conforming element is also easy to program as the closed-form expression of the corresponding finite element matrices can be found. However, the formulations of the GPL-T9 element were developed for bending analysis only for the plates under the applied mechanical loading. The finite element formulation for this element type under thermal loading, such as temperature gradient through the plate thickness, has not been found in any literature. The main objective of this paper is thus to present the formulation and the effectiveness of the GPL-T9 element in thermal bending analysis of thin plate.

The paper begins by presenting the governing differential equations for predicting the thin plate bending behaviors under the thermal loading. The corresponding finite element equations that include the element matrices with the thermal load vector are derived and presented. Several thin-plate thermal bending examples are used to evaluate the solution accuracy of the finite element formulation developed. Such solutions are also compared with those occurred from the well-known nonconforming triangular thin plate bending element (BCIZ) and the discrete Kirchhoff triangular element (DKT).

2. Governing Equations

The equation for the transverse deflection w in z -direction normal to the x - y plane of a thin plate with the temperature $T(z)$ through its thickness t is given by the equilibrium equation [11],

$$D \left(\frac{\partial^4 w}{\partial x^4} + 2 \frac{\partial^4 w}{\partial x^2 \partial y^2} + \frac{\partial^4 w}{\partial y^4} \right) = - \frac{1}{1-\nu} \left(\frac{\partial^2 M_T}{\partial x^2} + \frac{\partial^2 M_T}{\partial y^2} \right) + p(x, y) \quad (1)$$

CST0010

where $p(x,y)$ is the applied load normal to the x - y plane, ν is Poisson's ratio and D is the bending rigidity which can be defined as,

$$D = \frac{Et^3}{12(1-\nu^2)} \quad (2)$$

where E is the modulus of elasticity, t is the thickness of the plate. The thermal moment M_T in Eq. (1) is defined by,

$$M_T = E\alpha \int_{-t/2}^{t/2} (T(z) - T_0) z dz \quad (3)$$

3. Finite Element Equations

3.1 Generalized Conforming Element

To formulate a generalized conforming thin plate element, the modified potential energy theorem should be used as [12],

$$\Pi_{mp} = \Pi_p - \sum H = \text{stationary} \quad (4)$$

$$\begin{aligned} \Pi_p = \iint_{A_e} \frac{D}{2} \left[\left(\frac{\partial^2 w}{\partial x^2} \right)^2 + \left(\frac{\partial^2 w}{\partial y^2} \right)^2 + 2\nu \frac{\partial^2 w}{\partial x^2} \frac{\partial^2 w}{\partial y^2} \right. \\ \left. + 2(1-\nu) \left(\frac{\partial^2 w}{\partial x \partial y} \right)^2 \right] dx dy - \iint_{A_e} p w dx dy \quad (5) \end{aligned}$$

$$H = \int_{\partial A_e} \left[M_n \left(\frac{\partial w}{\partial n} + \tilde{\theta}_s \right) + M_{ns} \left(\frac{\partial w}{\partial s} - \frac{\partial \tilde{w}}{\partial s} \right) - Q_n (w - \tilde{w}) \right] ds \quad (6)$$

where Π_p and Π_{mp} are functions of minimum and modified potential energy theorems, respectively. H is the additional energy corresponding to the incompatible displacements on the element boundary ∂A_e in which Q_n , M_n and M_{ns} are Lagrange multipliers which denote the boundary tractions (transverse shear, normal moment and twisting moment) on the boundary ∂A_e , n and s denote the normal and tangential directions of the boundary, respectively. w is the deflection within the element. \tilde{w} is the boundary deflection of the element. And $\tilde{\theta}_s$ is the boundary rotation about the tangential axis s on ∂A_e .

In the limit as the size of the element tends to zero, the additional energy H is assumed to vanish such that,

$$H = \int_{\partial A_e} \left[M_n \left(\frac{\partial w}{\partial n} + \tilde{\theta}_s \right) + M_{ns} \left(\frac{\partial w}{\partial s} - \frac{\partial \tilde{w}}{\partial s} \right) - Q_n (w - \tilde{w}) \right] ds = 0 \quad (7)$$

Therefore, Π_{mp} degenerates to Π_p and the element stiffness matrix can be formulated on the basis of the degenerated form Π_p . The element so formulated is called a generalized conforming element.

In order to satisfy Eq. (7), we will first apply the formula of integration by parts and rewrite Eq. (7) as,

$$\begin{aligned} H = \int_{\partial A_e} \left[M_n \left(\frac{\partial w}{\partial n} + \tilde{\theta}_s \right) - \left(Q_n + \frac{\partial M_{ns}}{\partial s} \right) (w - \tilde{w}) \right] ds \\ + \sum_j (\Delta M_{ns})_j (w - \tilde{w})_j = 0 \quad (8) \end{aligned}$$

where j denotes the nodal point of the element and $(\Delta M_{ns})_j$ is the difference between the twisting moments acting at both sides of nodal point j . Then, the deflection field w is assumed to satisfy the following conditions,

$$(w - \tilde{w})_j = 0 \quad (\text{at each node } j) \quad (9)$$

$$\int_{S_k} (w - \tilde{w}) ds = 0 \quad (10)$$

$$\int_{S_k} \left(\frac{\partial w}{\partial n} + \tilde{\theta}_s \right) ds = 0 \quad (\text{on each side } S_k) \quad (11)$$

Equation (9) is the point compatibility condition for nodal deflection at each node. Other two equations, Eqs. (10) - (11), are the line compatibility conditions for average deflection and average normal slope along each side of the element. It is obviously that Eqs. (9) - (11) are a strong form of the condition Eq. (8).

3.2 The Generalized Conforming Triangular Element (GPL-T9)

A triangular thin-plate bending element with 9 DOF is shown in Fig. 1. The vector of nodal unknowns $\{\delta\}^e$ is defined as,

$$\{\delta\}^e = [w_1 \ \theta_{x1} \ \theta_{y1} \ w_2 \ \theta_{x2} \ \theta_{y2} \ w_3 \ \theta_{x3} \ \theta_{y3}]^T \quad (12)$$

where $\theta_{xi} = (\partial w / \partial x)_i$ and $\theta_{yi} = -(\partial w / \partial y)_i$ denote the nodal rotations.

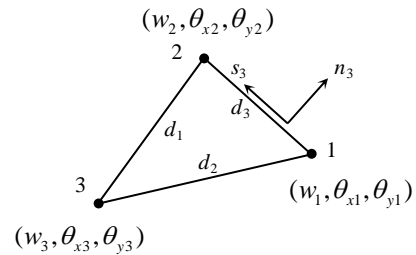


Fig. 1 Triangular plate bending element with 9 DOF

The deflection \tilde{w} and normal slope $\tilde{\theta}_s$ along side 12 are assume to be cubic and linear respectively as,

$$\begin{aligned} \tilde{w}_{12} = (L_1 + L_1^2 L_2 - L_2^2 L_1) w_1 - b_3 L_1^2 L_2 \theta_{x1} - c_3 L_1^2 L_2 \theta_{y1} \\ + (L_2 + L_2^2 L_1 - L_1^2 L_2) w_2 + b_3 L_2^2 L_1 \theta_{x2} + c_3 L_2^2 L_1 \theta_{y2} \quad (13) \end{aligned}$$

$$\tilde{\theta}_{s12} = \frac{1}{d_3} [L_1 (c_3 \theta_{x1} - b_3 \theta_{y1}) + L_2 (c_3 \theta_{x2} - b_3 \theta_{y2})] \quad (14)$$

CST0010

where L_i ($i = 1, 2, 3$) denotes area coordinates, d_i ($i = 1, 2, 3$) denotes the side length, and $b_3 = y_1 - y_2$ and $c_3 = x_2 - x_1$ are the coefficients appear in the area coordinates. Similar expressions for side 23 and 31 can be obtained by permutation.

Therefore, the deflection field w over the element can be express as follows,

$$w = w_1 L_1 + w_2 L_2 + w_3 L_3 + \hat{w} \quad (15)$$

and

$$\hat{w} = \lambda_1 L_1 L_2 + \lambda_2 L_2 L_3 + \lambda_3 L_3 L_1 + \lambda_4 F_4 + \lambda_5 F_5 + \lambda_6 F_6 \quad (16)$$

where

$$\begin{aligned} F_4 &= L_1(L_1 - 1/2)(L_1 - 1) \\ F_5 &= L_2(L_2 - 1/2)(L_2 - 1) \\ F_6 &= L_3(L_3 - 1/2)(L_3 - 1) \end{aligned} \quad (17)$$

It can be verified that the nodal compatibility condition Eq. (9) is already satisfied. The coefficients $\lambda_1, \lambda_2, \dots, \lambda_6$ in Eq. (16) are determined from the line compatibility condition Eqs. (10) and (11).

Consequently, the deflection field w can be rewritten in the form of,

$$w = [N] \{\delta\}^e = \sum_{i=1}^3 (N_i w_i + N_{xi} \theta_{xi} + N_{yi} \theta_{yi}) \quad (18)$$

where

$$\begin{aligned} N_1 &= L_1 - 2F_4 + (1-r_2)F_5 + (1+r_3)F_6 \\ N_{x1} &= -\frac{b_3}{2} L_1 L_2 + \frac{b_2}{2} L_3 L_1 - \frac{1}{2} (b_2 - b_3) F_4 \\ &\quad - \frac{1}{2} (r_2 b_2 + b_3) F_5 - \frac{1}{2} (r_3 b_3 - b_2) F_6 \\ N_{y1} &= -\frac{c_3}{2} L_1 L_2 + \frac{c_2}{2} L_3 L_1 - \frac{1}{2} (c_2 - c_3) F_4 \\ &\quad - \frac{1}{2} (r_2 c_2 + c_3) F_5 - \frac{1}{2} (r_3 c_3 - c_2) F_6 \end{aligned} \quad (19)$$

and

$$r_1 = \frac{d_2^2 - d_3^2}{d_1^2}, \quad r_2 = \frac{d_3^2 - d_1^2}{d_2^2}, \quad r_3 = \frac{d_1^2 - d_2^2}{d_3^2} \quad (20)$$

The expression for six other shape functions can be obtained by permutation. Based on these shape functions, the element stiffness matrix $[K]$ can be derived.

The finite element equations for thermal bending analysis of thin plate can be written in the form of,

$$[K] \{\delta\} = \{F_T\} + \{F_p\} \quad (21)$$

where $[K]$ is the element stiffness matrix, $\{\delta\}$ is the vector of the element nodal unknowns which contains transverse deflection and the rotations at each node, and $\{F_T\}$ is the equivalent nodal forces due to the thermal load associated with the temperature gradient through the plate thickness. While $\{F_p\}$ is the nodal force vector due to the applied lateral loads which is not considered in this study.

The element stiffness matrix $[K]$ is given by,

$$[K] = \iint_A [B]^T [D] [B] dA \quad (22)$$

where

$$[D] = \frac{Et^3}{12(1-\nu^2)} \begin{bmatrix} 1 & \nu & 0 \\ \nu & 1 & 0 \\ 0 & 0 & \frac{1-\nu}{2} \end{bmatrix} \quad (23)$$

and

$$[B] = \begin{bmatrix} -\left[\frac{\partial^2 N}{\partial x^2}\right] \\ -\left[\frac{\partial^2 N}{\partial y^2}\right] \\ -2\left[\frac{\partial^2 N}{\partial x \partial y}\right] \end{bmatrix} \quad (24)$$

The closed-form of the stiffness matrix can be written as,

$$[K] = [R]^T [Q] [R] \quad (25)$$

where the matrices $[R]$ and $[Q]$ is given in Appendix.

The vector of the equivalent nodal forces due to the thermal load $\{F_T\}$ in Eq. (21) can be derived by,

$$\{F_T\} = \frac{1}{1-\nu} \int_A [B]^T \{M\} dA \quad (26)$$

where the vector $\{M\}$ is given by,

$$\{M\}^T = [M_T \quad M_T \quad 0] \quad (27)$$

The thermal moment, M_T , in Eq. (27) is the function of the temperature through the plate thickness as defined in Eq. (3). The vector of the equivalent nodal thermal forces $\{F_T\}$ in Eq. (26) can be rewritten as,

$$\{F_T\} = \frac{1}{1-\nu} M_T \int_A [B]^T dx dy \begin{Bmatrix} 1 \\ 1 \\ 0 \end{Bmatrix} \quad (28)$$

CST0010

or

$$\{F_T\} = \frac{1}{1-\nu} M_T [BA] \begin{Bmatrix} 1 \\ 1 \\ 0 \end{Bmatrix} \quad (29)$$

where the closed-form of matrix $[BA]$ is shown in Appendix.

The closed-form expressions of the thermal load vector in Eq. (29) which have been derived in this study can be implemented for computer programming directly. The validity of the derived thermal load vector above is examined by thermal plate bending examples that have exact solutions as presented in the next section.

4. Applications

Three examples which have exact solutions are presented in this section. The first example is chosen to evaluate the performance of the GPL-T9 plate bending element. The other two problems demonstrate the effectiveness of the proposed element compared with the DKT and BCIZ triangular elements.

4.1 Free square plate

A square plate of which all edges are set to be free and the temperature varies linearly through the thickness is shown in Fig. 2. The plate is assumed to have the thickness (t) of 0.01 m, the modulus of elasticity (E) of 7.2×10^{10} N/m², the Poisson's ratio (ν) of 0.33, and the thermal expansion coefficient (α) of 2.3×10^{-7} /°C. The plate has the temperatures of the upper surface (T_U) of 100 °C and the lower surface (T_L) of 25 °C. The exact transverse deflection (w) of free square plate with linear temperature distribution through its thickness can be derived [13] and is given by,

$$w(x, y) = -\frac{\alpha \Delta T}{2t} (x^2 + y^2) \quad (30)$$

where ΔT is the temperature difference between upper and lower surface.

Due to its symmetry, only the top right quarter of the plate is modeled and analyzed. The finite element model for this problem is illustrated in Fig. 3. The model is divided to 4x4 intervals consisted of uniform meshes with 25 nodes and 32 elements. Figure 4 shows the predicted transverse deflections along the x -axis obtained from GPL-T9 element. It can be seen that the results obtained from the proposed element are definitely the same as the exact solution at any points of nodes. This shows the performance of the GPL-T9 element that can accurately predict the transverse deflections of the plate due to temperature gradient through its thickness.

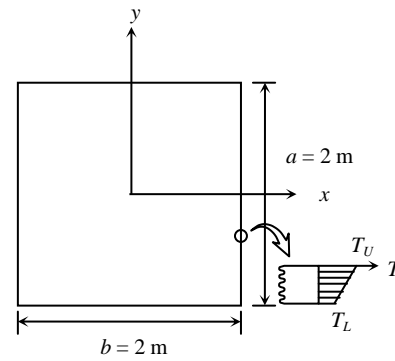


Fig. 2 Free square plate with linear temperature gradient through its thickness.

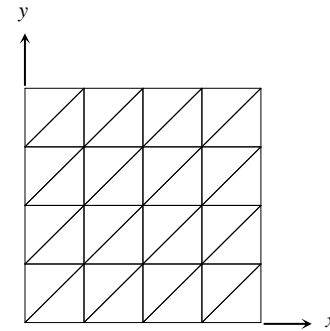


Fig. 3 Finite element meshes of free square plate

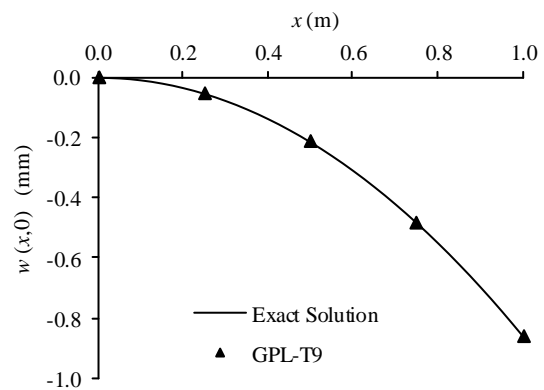


Fig. 4 Comparative transverse deflections along x -axis

4.2 Clamped and simply supported rectangular plate

The clamped and simply supported rectangular plate of which the temperature varies linearly along the thickness only is considered. This plate is clamped along the edges $y = \pm b/2$ and simply supported along the edges $x = 0$ and $x = a$ as shown in Fig. 5. The derivation for the exact solution of the deflection (w) is given in Ref. [14] as,

$$w(x, y) = \sum_{m=1,3,5}^{\infty} (A_m \cosh \alpha_m y + D_m y \sinh \alpha_m y + K_m) \sin \alpha_m x \quad (31)$$

where α_m, A_m, D_m, K_m and Δ_m are,

CST0010

$$\alpha_m = \frac{m\pi}{a} \quad (32)$$

$$A_m = -K_m \left(\frac{1}{2} \alpha_m b \cosh \frac{1}{2} \alpha_m b + \sinh \frac{1}{2} \alpha_m b \right) / \Delta_m \quad (33)$$

$$D_m = K_m \alpha_m \left(\sinh \frac{1}{2} \alpha_m b \right) / \Delta_m \quad (34)$$

$$K_m = \frac{4M_T}{aD\alpha_m^3} \quad (35)$$

$$\Delta_m = \frac{1}{2} \alpha_m b + \sinh \frac{1}{2} \alpha_m b \cosh \frac{1}{2} \alpha_m b \quad (36)$$

while D and M_T are given in Eqs. (2) and (3), respectively.

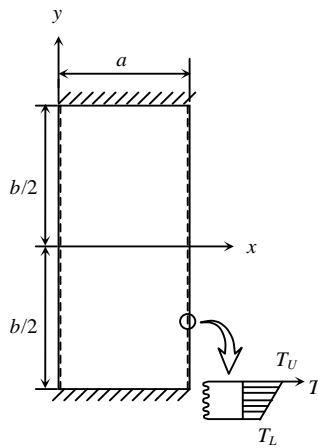


Fig. 5 Clamped and simply supported rectangular plate with linear temperature gradient through its thickness.

In this example, the geometric properties of plates are the width (a) = 2 m, the length (b) = 4 m, and the thickness (t) = 0.01 m. The physical properties of the plate are taken as the modulus of elasticity (E) of 190 GPa, the Poisson's ratio (ν) of 0.3, and the thermal expansion coefficient (α) of $16 \times 10^{-6} / ^\circ\text{C}$. The temperatures of the upper surface (T_U) and the lower surface (T_L) of the plate are 60°C and 0°C , respectively.

Since the problem is symmetrical, a quarter of the plate is analyzed. The models consist of the uniform 4x8, 8x16 and 16x32 mesh divisions which have 45 nodes, 153 nodes and 561 nodes, respectively. The example of finite element models using in the analysis is shown in Fig. 6. The deflections at the plate center (w_c) obtained in the present analysis are illustrated in Fig. 7. It can be seen that the results obtained from all element types converge to the exact solution as the meshes are refined. The results show that the GPL-T9 element performs very well and provides higher solution accuracy than other element types.

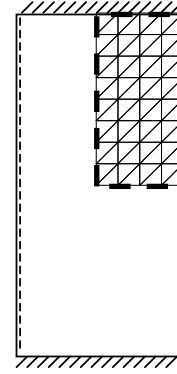


Fig. 6 The 4x8 finite element meshes of the clamped and simply supported rectangular plate.

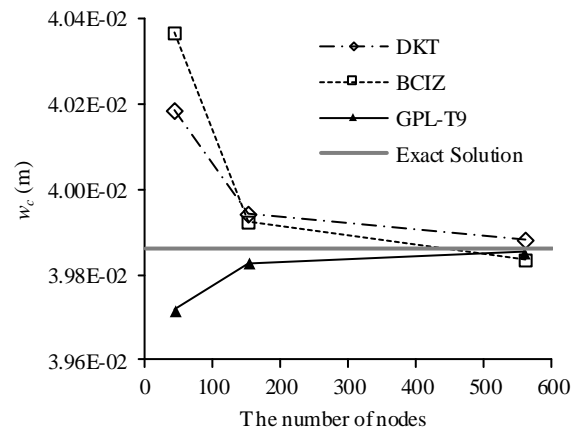


Fig. 7 Predicted central deflections of the clamped and simply supported rectangular plate compared with the exact solution.

4.3 Simply supported parallelogram plate

A problem statement of the simply supported parallelogram plate with linear temperature gradient through its thickness is shown in Fig. 8. The dimensions of the plate in the analysis are $a = 2$ m, $b = 1$ m and $\gamma = 30^\circ$. The plate is assumed to have the modulus of elasticity (E) of 190 GPa, the Poisson's ratio (ν) of 0.3, the thermal expansion coefficient (α) of $16 \times 10^{-6} / ^\circ\text{C}$, the thickness (t) of 0.01 m, the upper surface temperature (T_U) of 60°C , and the lower surface temperature (T_L) of 0°C . The exact central transverse deflection (w_c) of the simply supported parallelogram plate for $a/b = 2$ and $\gamma = 30^\circ$ is given by [15],

$$w_c = 0.090135 \frac{M_T b^2}{D} \quad (37)$$

CST0010

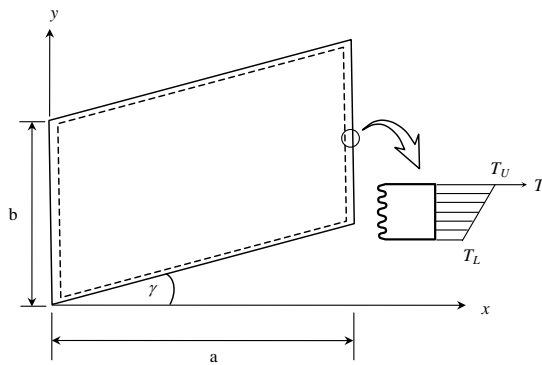


Fig.8 Simply supported parallelogram plate with linear temperature gradient through its thickness.

where D and M_T are the same as written in Eqs. (2) and (3), respectively.

The model is discretized into uniform meshes of 8×4 (45 nodes), 16×8 (153 nodes) and 20×10 (231 nodes) intervals as illustrated in Fig. 9 (a)-(c). The predicted central transverse deflections compared with the exact solution are shown in Fig. 10. The results indicate that both DKT and GPL-T9 elements apparently provides good solution accuracy while the solution obtained from the non-conforming BCIZ element diverges from the exact solution.

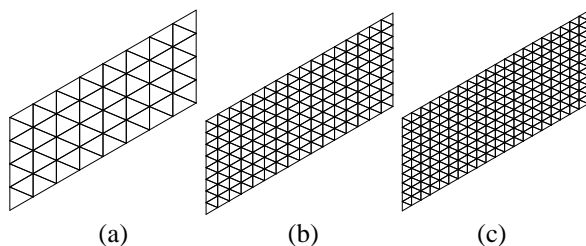


Fig.9 Finite element meshes of parallelogram plate.

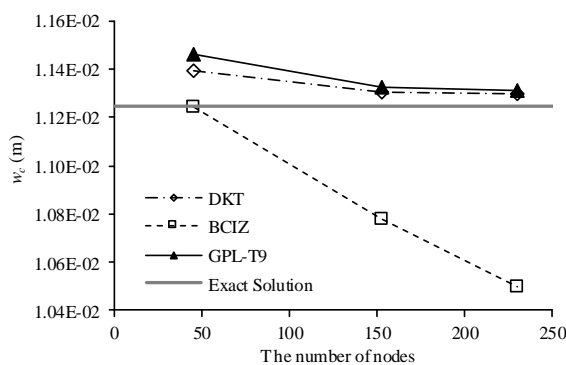


Fig.10 Predicted central deflections of the simply supported parallelogram plate compared with the exact solution.

5. Conclusion

The generalized conforming triangular element for plate bending analysis with the temperature gradient through its thickness was presented. The finite element formulation with detailed finite element matrices were derived based on the modified potential energy principle and the generalized compatibility

conditions. The finite element stiffness matrix and the equivalent nodal forces due to the thermal load of the GPL-T9 plate bending element were derived and rewritten in closed-form which can be used in computer programming directly. The presented examples demonstrated that the generalized conforming plate bending element GPL-T9 with the proposed thermal load formulation provides good solution accuracy in thermal bending analysis of thin plate. The results obtained from the proposed element also converge to the exact solution when the mesh is refined. The solution accuracy obtained from both DKT and GPL-T9 elements is quite in the same high quality; however, the GPL-T9 is better when we consider in the simplicity of its formulation. Moreover, the non-conforming plate bending element BCIZ is somehow unreliable in some cases as we have seen in the third example that it gives diverged solution.

6. References

- [1] Hrabok, M.M. and Hrudey, T.M. (1984). A review and catalogue of plate bending finite elements, *Computers & Structures*, Vol.19(3), 1984, pp. 479-495.
- [2] Mackerle, J. (1995). Static and Dynamic Analysis of Plates Using Finite Element and Boundary Elements - a Bibliography (1992-1994), *Finite Elements in Analysis and Design*, Vol.20(2), 1995, pp. 139-154.
- [3] Batoz, J.L., Bathe, K.J. and Ho, L.W. (1980). A Study of Three-node Triangular Plate Bending Elements, *International Journal for Numerical Methods in Engineering*, Vol.15(12), 1980 pp. 1771-1812.
- [4] Batoz, J.L., Zheng, C.L. and Hammadi, F. (2001). Formulation and evaluation of new triangular, quadrilateral, pentagonal and hexagonal discrete Kirchhoff plate/shell elements, *International Journal for Numerical Methods in Engineering*, Vol. 52(5-6), 2001, pp. 615-630.
- [5] Bazeley, G.P., Cheung, Y.K., Irons, B.M. and Zienkiewicz, O.C. (1965). Triangular Elements in Plate Bending Conforming and Non-conforming Solution, *Proceedings 1st Conference on Matrix Methods in Structural Mechanics*, Air Force Ins. Tech., Wright-Patterson A.F. Base, Ohio, United States, pp. 547-576.
- [6] Zienkiewicz, O.C. and Taylor, R.L. (2005). *The Finite Element Method for Solid and Structural Mechanics*, 6th edition, Elsevier Butterworth-Heinemann, Oxford, 2005.
- [7] Bhothikhun, P. and Dechaumphai, P. (2014). Adaptive DKT Finite Element for Plate Bending Analysis of Built-up Structures, *International Journal of Mechanical & Mechatronics Engineering*, Vol.14(1), 2014, pp. 12-20.
- [8] Bhothikhun, P. and Dechaumphai, P. (2015). Development of DKT Finite Element Formulation for Thermal Bending of Thin Plate, *Journal of Thermal Stresses*, Vol.38(7), 2015, pp. 775-791.

CST0010

[9] Zhifei, L. (1993). Generalized conforming triangular elements for plate bending, *Communications in Numerical Methods in Engineering*, Vol.9(1), January 1993, pp. 53-65.

[10] Yuqiu, L., Xiaoming, B., Zhifei, L. and Yin, X. (1995). Generalized conforming plate bending elements using point and line compatibility conditions, *Computers & Structures*, Vol.54(4), 1995, pp.717-723.

[11] Dechaumphai, P. (2010). *Finite Element Method: Fundamentals and Applications*, Alpha Science International, Oxford.

[12] Yuqiu, L. and Kegui, X. (1987). The generalized conforming element, *China Civil Engineering Journal*, Vol.20(1), 1987, pp. 1-14.

[13] Boley, B.A. and Weiner, J.H. (1997), *Theory of Thermal Stresses*, Dover Publications, New York.

[14] Hetnarski, R.B. (2014). *Encyclopedia of Thermal Stresses*, Springer, New York.

[15] Kulakov, V.M., Uspenskii, A.A. and Frolov, A.N. (1975). Thermal Deflection in a Parallelogram Plate, *Strength of Materials*, Vol.7(11), 1975, pp. 1362-1364.

7. Appendix

The closed-form of the stiffness matrix $[K]$ is given in Eq. (25) as,

$$[K] = [R]^T [Q] [R] \quad (A1)$$

where the matrices $[R]$ and $[Q]$ is defined by,

$$[R] = [C][A] \quad (A2)$$

$$[C] = -\frac{1}{4A^2} \begin{bmatrix} 2b_1b_2 & 2b_2b_3 & 2b_3b_1 & 3b_1^2 & -3b_2^2 & -3b_3^2 \\ 2b_1b_2 & 2b_2b_3 & 2b_3b_1 & -3b_1^2 & 3b_2^2 & -3b_3^2 \\ 2b_1b_2 & 2b_2b_3 & 2b_3b_1 & -3b_1^2 & -3b_2^2 & 3b_3^2 \\ 2c_1c_2 & 2c_2c_3 & 2c_3c_1 & 3c_1^2 & -3c_2^2 & -3c_3^2 \\ 2c_1c_2 & 2c_2c_3 & 2c_3c_1 & -3c_1^2 & 3c_2^2 & -3c_3^2 \\ 2c_1c_2 & 2c_2c_3 & 2c_3c_1 & -3c_1^2 & -3c_2^2 & 3c_3^2 \\ 2(b_1c_2 + b_2c_1) & 2(b_2c_3 + b_3c_2) & 2(b_3c_1 + b_1c_3) & 6b_1c_1 & -6b_2c_2 & -6b_3c_3 \\ 2(b_1c_2 + b_2c_1) & 2(b_2c_3 + b_3c_2) & 2(b_3c_1 + b_1c_3) & -6b_1c_1 & 6b_2c_2 & -6b_3c_3 \\ 2(b_1c_2 + b_2c_1) & 2(b_2c_3 + b_3c_2) & 2(b_3c_1 + b_1c_3) & -6b_1c_1 & -6b_2c_2 & 6b_3c_3 \end{bmatrix} \quad (A3)$$

$$[A] = \begin{bmatrix} 0 & -\frac{1}{2}b_3 & -\frac{1}{2}c_3 & 0 & \frac{1}{2}b_1 & \frac{1}{2}c_1 & 0 & 0 & 0 \\ 0 & 0 & 0 & 0 & -\frac{1}{2}b_1 & -\frac{1}{2}c_1 & 0 & \frac{1}{2}b_2 & \frac{1}{2}c_2 \\ 0 & \frac{1}{2}b_2 & \frac{1}{2}c_2 & 0 & 0 & 0 & 0 & -\frac{1}{2}b_3 & -\frac{1}{2}c_3 \\ -2 & -\frac{1}{2}(b_2 - b_1) & -\frac{1}{2}(c_2 - c_1) & 1 + \nu & -\frac{1}{2}(b_1 - b_2) & \frac{1}{2}(c_1 - c_2) & 1 - \nu & \frac{1}{2}(b_1 + b_2) & -\frac{1}{2}(c_1 + c_2) \\ 1 - \nu & -\frac{1}{2}(b_2 + b_1) & -\frac{1}{2}(c_2 + c_1) & -2 & -\frac{1}{2}(b_1 - b_2) & -\frac{1}{2}(c_1 - c_2) & 1 + \nu & \frac{1}{2}(b_2 - b_1) & -\frac{1}{2}(c_2 - c_1) \\ 1 + \nu & -\frac{1}{2}(b_1 - b_2) & -\frac{1}{2}(c_1 - c_2) & 1 - \nu & -\frac{1}{2}(b_2 + b_1) & -\frac{1}{2}(c_2 + c_1) & -2 & -\frac{1}{2}(b_1 - b_2) & -\frac{1}{2}(c_1 - c_2) \end{bmatrix} \quad (A4)$$

$$[Q] = \frac{Et^3}{12(1-\nu^2)} \begin{bmatrix} [P] & \nu[P] & [0] \\ \nu[P] & [P] & [0] \\ [0] & [0] & \frac{1-\nu}{2}[P] \end{bmatrix} \quad (A5)$$

$$[P] = \frac{A}{12} \begin{bmatrix} 2 & 1 & 1 \\ 1 & 2 & 1 \\ 1 & 1 & 2 \end{bmatrix} \quad (A6)$$

The vector of the equivalent nodal thermal forces $\{F_T\}$ is given in Eq. (29) as,

$$\{F_T\} = \frac{1}{1-\nu} M_T [BA] \begin{Bmatrix} 1 \\ 1 \\ 0 \end{Bmatrix} \quad (29)$$

where the closed-form of matrix $[BA]$ is in the form of,

$$[BA] = [A]^T [T] \quad (A7)$$

$$[T] = \frac{1}{4A} \begin{bmatrix} -2b_1b_2 & -2c_1c_2 & -2(b_1c_2 + b_2c_1) \\ -2b_2b_3 & -2c_2c_3 & -2(b_2c_3 + b_3c_2) \\ -2b_3b_1 & -2c_3c_1 & -2(b_3c_1 + b_1c_3) \\ b_1^2 & c_1^2 & 2b_1c_1 \\ b_2^2 & c_2^2 & 2b_2c_2 \\ b_3^2 & c_3^2 & 2b_3c_3 \end{bmatrix} \quad (A8)$$